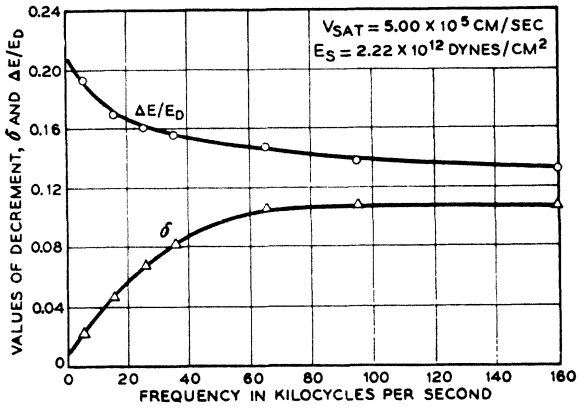

FIG. 1. Values of decrement and $\Delta E/E_D$ plotted as a function of frequency.

The change in intensity of magnetization associated with the domain wall motion is $I=\frac{2}{3}I_s/D$, so that the susceptibility is

$$\chi_0=I/H=I_s^2/3K'D, \quad \text{or} \quad K'=I_s^2/3\chi_0 D, \tag{3}$$

where D is the domain thickness in the direction of domain motion.

The power loss for a 180° wall has been calculated[2] by Williams, Shockley, and Kittel for a domain whose cross-sectional area is large compared with its thickness. The loss in a 90° wall will be $\frac{1}{4}$ of this; and if we equate this power loss to the rate at which the energy is supplied, we have

$$16D^2I_s^2v^2/\pi R=HI_svD, \quad \text{or} \quad v=\pi RH/16DI_s, \tag{4}$$

where R is the resistivity of the material and v the velocity of the wall. From Eq. (1), if the dissipative term is controlling, we obtain

$$dx/dt=v=HI_s/R'; \quad \text{hence} \quad R'=16DI_s^2/\pi R. \tag{5}$$

Hence, from Eqs. (1), (2), and (3) the complex susceptibility is

$$\chi=\chi_0/[1+jf/f_0],$$

where f_0, the relaxation frequency, is

$$f_0=K'/2\pi R'=R/96\chi_0D^2=\pi R/24\mu_0D^2, \tag{6}$$

μ_0 being the initial permeability. This is the same relaxation frequency as that obtained by calculating the eddy current shielding for a plate the same thickness as the domain.

It is difficult to observe this relaxation of the domain wall motion magnetically, since it is obscured by eddy current damping of the whole specimen. However, by using domain wall movements caused by mechanical stresses, no over-all flux is generated and as shown by Fig. 1, this relaxation can be observed. The magnitude

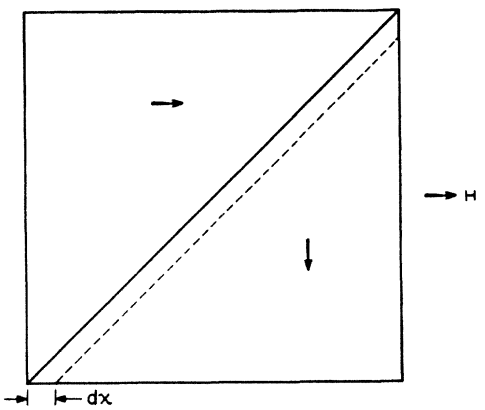

FIG. 2. Domain wall motion for a 90° domain wall.

of the change in the elastic constant (ΔE) and the damping can be calculated by inserting the complex value of the susceptibility in Becker and Döring's expression[3] for the ΔE effect. This results in

$$\Delta E/E_D=9\lambda^2E_s\mu_0/20\pi I_s^2(1+jf/f_0)$$
$$=9\lambda^2E_s\mu_0(1-jf/f_0)/20\pi I_s^2(1+f^2/f_0^2). \tag{7}$$

The real part of this equation represents the difference between the saturated Young's modulus E_s and the demagnetized Young's modulus, E_D, as a function of frequency. The imaginary part represents the dissipation associated with the domain wall motion, and the "Q" of the motion is given by taking the ratio of the real and imaginary parts of the complete elastic constant, i.e., $E_s-\Delta E$. Since the decrement δ is π/Q, we have

$$\delta=\frac{9}{20}\left(\frac{\mu_0\lambda^2E_s}{I_s^2}\right)\left(\frac{f/f_0}{1+f^2/f_0^2}\right). \tag{8}$$

The 90° wall model does not represent nickel, which has its easy direction of magnetization along the [111] directions. Döring,[4] in considering the $\Delta E/E_D$ effect, has shown that the result of this modification is to replace $(3/2)\lambda$ by $\lambda_{111}[5c_{44}/(c_{11}-c_{12}+3c_{44})]$, where λ_{111} is the magnetostrictive constant along [111] direction and c_{11}, c_{12}, and c_{44} are the three elastic constants of nickel. For $\lambda_{111}=-25\times10^{-6}$, $I_s=484$, $c_{11}=2.53\times10^{12}$ dynes/cm^2, $c_{12}=1.58\times10^{12}$, $c_{44}=1.23\times10^{12}$, and the measured values of $\mu_0=340$ and $E_s=2.22\times10^{12}$ dynes/cm^2, the calculated low frequency value of $\Delta E/E_D$ is 0.224 and the maximum value of δ is 0.353. From the initial slope, $\delta/f=2.5\times10^{-6}$ and the frequency of maximum decrement $f_0=150{,}000$ cycles, the average domain size is about 0.05 mm. The actual shape of the $\Delta E/E_D$ curve of Fig. 1 indicates a distribution of domain sizes from 0.15 mm to 0.02 mm, which is in good agreement with the optical measurements of Williams.[5]

I wish to thank Dr. R. M. Bozorth and Dr. C. Kittel for helpful conversations.

[1] Bozorth, Mason, and McSkimin, Phys. Rev. **83**, 220 (A) (1951). A fuller account is to be published in the October issue of the *Bell System Technical Journal*.
[2] Williams, Shockley, and Kittel, Phys. Rev. **80**, 1090 (1950).
[3] M. Becker and W. Döring, *Ferromagnetismus* (Verlag. Julius Springer, Berlin, 1930), p. 343.
[4] W. Döring, Z. Physik **114**, 579 (1939).
[5] H. J. Williams, to be published.

Electron Penetration and Scattering in Phosphors

L. R. KOLLER AND E. D. ALDEN
General Electric Research Laboratory, Schenectady, New York
(Received May 15, 1951)

THERE is very little experimental data on the loss of energy of electrons in phosphors. The availability in this laboratory of thin uniform chemically deposited layers of phosphors afforded an opportunity of making such measurements. The preparation of these films of zinc sulfide is described in a Letter to the Editor.[1] The films studied were deposited on glass and varied in thickness from about 0.1 to 0.45 micron.

The samples were excited by electron bombardment at voltages from 2 to 40 kv in a demountable post accelerator cathode-ray tube. A film of aluminum 0.01μ thick was evaporated onto the surface of the phosphor to prevent "sticking." Corrections were made for the energy lost by the electrons in this layer. The brightness at constant beam current (current density 0.8 μa/cm^2) as a function of beam voltage was measured with a photomultiplier tube. These quantities were displayed on a cathode-ray oscilloscope and the resulting trace photographed.

A typical voltage brightness relation is shown in Fig. 1. After the initial portion of the curve (not shown here) over which the brightness increases as a power of the voltage, there is a considerable range over which the brightness is a linear function of voltage, after which it passes through a fairly sharp maximum. The point at which the relation deviates from a straight line is interpreted

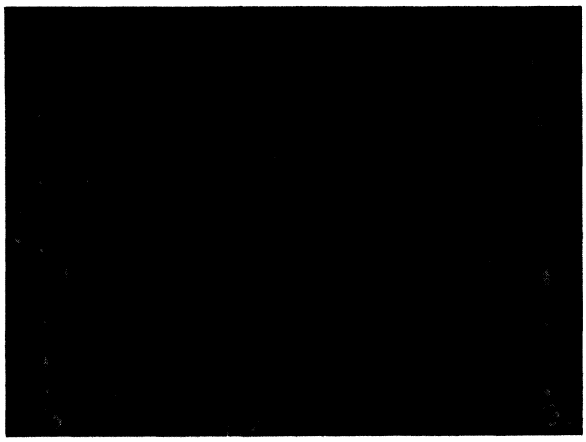

FIG. 1. A typical voltage-brightness relation. The abscissa is the beam voltage in kv, and the ordinate is the photocurrent.

as the voltage at which electrons pass completely through the phosphor and begin to give up energy in the glass. In the Thompson-Whiddington relation

$$V_0^2 - V^2 = bx,$$

where V_0 = initial energy in electron volts, and V = energy after traveling a distance x, the value of b calculated on this basis is 5.5 kv²/cm.

Since electrons are scattered in passing through the medium, the beam intensity must decrease with depth, and the law of beam energy as a function of depth of penetration in the medium becomes

$$E = i_0[(V_0^2 - bx)/V_0^2]^{\frac{1}{2}+a/b},$$

where a is the scattering constant defined by

$$-dN/dx = N^a/V^2,$$

where N is the number of electrons in the beam. The value of a/b determined for ZnS is 2.4. These results indicate a large initial rate of loss of energy by an electron beam passing through a phosphor. Nearly 90 percent of the beam energy is lost in a distance of half the range of the electrons.

[1] Studer, Cusano, and Young, J. Opt. Soc. Am. (to be published).

On the Lifetime of the Negative Pi-Meson*

L. M. LEDERMAN, E. T. BOOTH, H. BYFIELD, AND J. KESSLER
Department of Physics, Columbia University, New York, New York
(Received June 20, 1951)

THREE determinations of the lifetime of the positive pi-meson have recently been made.[1-3] All of these values are significantly higher than the lifetime obtained for negative pi-mesons by Richardson,[4] who first measured this quantity with cyclotron-produced particles. A summary of the reported results is given in Table I.

TABLE I. Summary of π-meson lifetimes.

Author	Meson	Lifetime
Martinelli and Panofsky	π^+	$1.97\,^{+0.21}_{-0.25}\times10^{-8}$ sec
Kraushaar, Thomas, and Henri	π^+	$1.65\pm0.33\times10^{-8}$ sec
Chamberlain, Mozley, Steinberger, and Wiegand	π^+	$2.65\pm0.12\times10^{-8}$ sec
Richardson	π^-	$1.11\,^{+0.45}_{-0.35}\times10^{-8}$ sec

The negative pi-meson lifetime has been redetermined, using the external meson beam of the Nevis cyclotron. The competition of nuclear capture prevents the application of the elegant electronic techniques employed by Chamberlain *et al.* and Kraushaar *et al.* with positive mesons, stopping in scintillation crystals. Instead, the decays are observed in the course of the flight of pi-mesons through a 16 in. magnet cloud chamber. To verify that the process $\pi^- \rightarrow \mu^- + \nu^0$ is actually the mechanism responsible for the negative pi-meson decays observed in the cloud chamber, the previously reported[5] momentum and angle analyses were extended to seventy-five events occurring in favorable regions of the chamber. These gave, for the mass of the neutral decay product, $m_{\nu^0} < 30m_e$. If the neutrino rest mass is taken as zero, the mu minus mass obtained from these data is

$$M_{\mu^-} = 209.8\pm2.2m_e,$$

where the pi-meson mass is taken as $276.1\pm1.3m_e$.[6]

The mean free path for $\pi \rightarrow \mu$ decay was obtained from the total length of pi-meson track classified as acceptable flux and the corrected number of decay events observed. Particles were allowed as flux if they entered the cloud chamber within a cone of 70° with respect to a fixed reference direction. The momentum interval accepted was 130 to 170 Mev/c. In order to minimize the subjectivity of the flux count, no restriction was placed on the quality of illumination of the track. Instead, all beam tracks were followed until they passed through the chamber or out of the illuminated region.

To reduce the possibility of mistaking a distorted track for a decay, the region of the cloud chamber in which events were counted was rigidly prescribed to be one inch from all vertical surfaces. The flux was then corrected for the reduced path during which decays would be recorded. A map measurer was employed on a full-scale reprojection of the cloud chamber photographs to obtain the actual lengths of the flux tracks.

Decays through angles whose projection is less than 5° in either of the two stereoscopic cameras were not counted. This procedure served to avoid the difficulty of determining the efficiency of stereoscopic scanning for decay events. The correction for the number of decays through angles $<5°$ was made from the geometry of the camera system and the calculated angular distribution of the decays. This yielded 0.33 ± 0.03 as the fraction of $\pi \rightarrow \mu$ decays excluded by the 5° criterion. Finally, a correction was made for the fraction of acceptable flux particles which are not pi-mesons.

The contaminants consist of mu-mesons and electrons. The electron contribution was estimated from the number of multiplication events observed in a 0.6 radiation length lead plate. This was independently checked by the electronic time-of-flight counter telescope.[7] The resultant electron fraction, 10 ± 3 percent, is roughly consistent with that to be expected from the materialization of π^0 decay photons in the $4\times4\times\frac{1}{2}$ in. Be target. The mu-component was determined by an electronic mu-meson detector[8] (counting delayed coincidences between the mu-meson and its decay electron), which yielded a range spectrum of mu-mesons with a geometry designed to simulate that of the cloud chamber. The number of mu's in the proper momentum interval was found to be 9 ± 3 percent.

The mean free path for decay in the laboratory system, based on 188 events, is 9.93 ± 1.10 meters. The error represents the uncertainties in beam composition, efficiency, and statistics, assumed to enter independently. This corresponds to a laboratory mean life of $4.55\pm0.52\times10^{-8}$ second. If the mean free path is reduced to the rest system lifetime by the time dilation factor of special relativity, $\langle m/cp\rangle_{Av}$, averaged over the momentum spectrum of flux particles, the result is

$$\tau_{\pi^-} = 2.92\pm0.32\times10^{-8} \text{ second}$$

in satisfactory agreement with the more recent[3] determinations of the positive mean life.

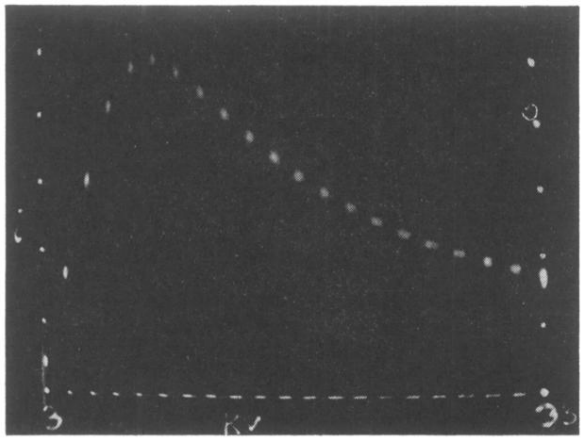

FIG. 1. A typical voltage-brightness relation. The abscissa is the beam voltage in kv, and the ordinate is the photocurrent.